

Measuring the physical conditions of accreting gas in T Tauri systems

Jeffrey S. Bary¹ and Sean P. Matt¹

¹Department of Astronomy, University of Virginia, Charlottesville, VA 22902, USA
email: jbary@virginia.edu, spm5x@virginia.edu

Abstract. Hydrogen emission lines observed from T Tauri stars (TTS) are associated with the accretion/outflow of gas in these young star forming systems. Magnetospheric accretion models have been moderately successful at reproducing the shapes of several H I emission line profiles, suggesting that the emission arises in the accretion funnels. Despite considerable effort to model and observe these emission features, the physical conditions of the gas confined to the funnel flows remain poorly constrained by observation. We conducted a multi-epoch near-infrared spectroscopic survey of 16 actively accreting classical TTS in the Taurus-Auriga star forming region. We present an analysis of these *simultaneously* acquired line flux ratios of many Paschen and Brackett series emission lines, in which we compare the observed ratios to those predicted by the Case B approximation of hydrogen recombination line theory. We find that the line flux ratios for the Paschen and Brackett decrements as well as a comparison between Br γ and Paschen transitions agree well with the Case B models with $T < 5000$ K and $n_e \approx 10^{10}$ cm⁻³.

Keywords. Accretion, stars: low-mass, formation, variables: T Tauri stars, infrared: stars

1. HI forms in accretion flows?

Where and how the neutral hydrogen emission lines are formed in the environment of accreting T Tauri stars remains an outstanding problem. Initially, the hydrogen lines were associated with stellar winds and mass loss. However, in the last ten to fifteen years we have witnessed a sea-change in this interpretation and the H I lines have come to *signify* accretion, as the concept of magnetospherically guided accretion (Ghosh & Lamb 1979; Königl 1991; Shu *et al.* 1994) has gained wide acceptance, partly due to its success at explaining the line shapes of some of the Balmer series, Pa β , and Br γ emission lines (Hartmann *et al.* 1994; Muzerolle *et al.* 1998a, 2001).

Balmer series lines appear quite complicated, displaying a variety of structures which vary from star-to-star and from epoch-to-epoch (Basri & Batalha 1990). On the other hand, the infrared Paschen and Brackett series features, with their lower opacity may not experience the same self-absorption or other complicating optical depth effects. Folha & Emerson (2001) collected high resolution near-infrared spectra of 50 TTS to study the Pa β and Br γ emission lines and found what they described as a 'conspicuous' lack of blueshifted absorption features. The absence of blueshifted absorption in the infrared lines may imply that they are not produced in an outflowing wind. However, this work and others (e.g., Johns & Basri 1995; Alencar & Basri 2000), that have conducted large scale high resolution surveys of H I conclude that much work needs to be done to determine if the observed H I line shapes can be accurately modeled by the magnetospheric accretion model. For the purpose of discussion, in these proceedings we make the initial assumption that the H I gas emission is produced in the accretion column.

2. The need for simultaneous observations

Previous attempts to determine the temperature of the emitting HI gas using line ratios have been inconclusive with the measured values not agreeing with those expected for optically thick or thin gas in local thermodynamic equilibrium. Additionally, comparisons of these ratios to those predicted by the Case B approximation of Baker *et al.* (1938) recombination line theory, likewise have proven unsuccessful. However, in most cases the line ratio, usually only $\text{Pa}\beta/\text{Br}\gamma$, was determined from spectra collected at different times. Given the short timescale variability (on the order of hours) that has been observed for the fluxes of these individual lines, a line ratio calculated from two observations separated by a day or more will easily vary significantly from a value determined from spectra taken simultaneously. Therefore, it is not surprising that the line ratio comparisons have failed to contribute anything meaningful to our understanding of the physical conditions of the accreting gas.

The lack of agreement between the measured and predicted line ratios have lead astronomers to conclude that the emitting region is quite complicated. We suggest that this interpretation of the extant line flux data may be non-sensical given the variability of the emission features and the lack of simultaneous observations. In order to address the shortcomings of the previous line ratio comparisons, we present an analysis of multiple near-infrared HI line ratios measured from 104 multi-epoch spectral observations of 16 actively accreting cTTS in the Taurus-Auriga star forming region. The excellent wavelength coverage of CorMASS, a cross-dispersed low resolution ($R\sim 300$) spectrometer with continuous coverage from 0.8 to 2.5 μm , allows us to *simultaneously* measure the strength of any detectable HI emission feature in both the Paschen and Brackett series. The data improve upon previous analyses, not only by acquiring the line data at the same time, but by increasing the number of line ratios and range of n -states included in the analysis.

3. Simultaneous spectral observations

The survey spectra were collected using CorMASS on the 1.8m Vatican Advanced Technology Telescope (VATT) atop Mt. Graham, AZ over a two year period beginning in December 2003 and ending January 2005. On VATT, CorMASS slit dimensions are $1''6$ in width and $12''2$ in length. Observations of both the target cTTS and telluric calibration sources were made using a standard ABBA nod procedure to allow for efficient removal of sky background, sky emission lines, and dark current. Standard data reduction was performed using the IDL program CORMASSTOOL, which was adapted from SpexTOOL (Cushing *et al.* 2004). As an illustration of the wavelength coverage and the information included in the CorMASS spectra, we include Figure 1, which contains ten epochs of observations of DR Tau.

4. Measuring HI line ratios

We measured line fluxes for nine Paschen ($\text{Pa}\beta$, γ , δ , 8, 9, 10, 11, 12, and 14) and eight Brackett series ($\text{Br}\gamma$, 10, 11, 12, 13, 14,15, and 16) lines. Single-epoch observations of all sources show a broad range of HI line fluxes for the entire sample, while multi-epoch observations of the individual sources find significant variability in these same features. Since it has been shown that a correlation likely exists between the strength of the infrared HI line fluxes and the mass accretion rates of TTS (Skrutskie *et al.* 1996; Muzerolle *et al.* 1998b), our spectral observations sample a set of actively accreting TTS with a variety of mass accretion rates.

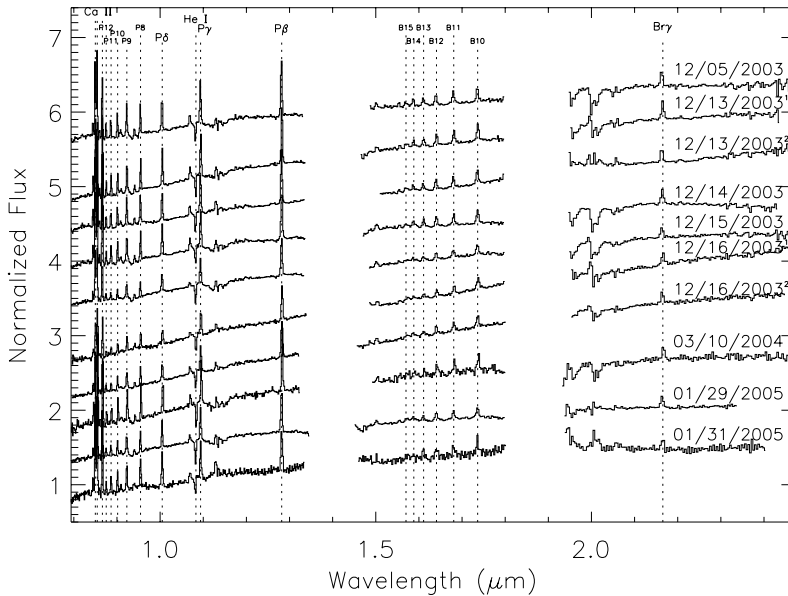


Figure 1. As an example of the spectra taken for the multi-epoch survey, we present all of the spectra obtained for the source, DR Tau. Each spectrum contains multiple HI recombination emission features, the Ca II infrared triplet in emission, and the He I ($1.083 \mu\text{m}$) feature, seen here in absorption. Individual spectra are labeled with the UT date on which it was observed. Vertical dotted lines locate the spectral features. Note that telluric water features have been removed near 1.4 and $1.9 \mu\text{m}$.

In Figure 2, we plot all of the dereddened line fluxes measured for $\text{Pa}\gamma$ against those measured for $\text{Pa}\beta$, including errors, and find there to be a strong correlation between the two. Surprisingly, we find little variation in the line ratios from source-to-source and for different epochs of observations of the same source where even the most substantial fluctuations in line strengths were observed. If these line fluxes are, indeed, correlated with mass accretion rate, this result suggests that the line ratios are insensitive to the mass accretion rate and one ‘global’ $\text{Pa}\gamma/\text{Pa}\beta$ ratio may be determined for all the stars in our survey.

In order to find a representative ‘global’ line ratio, we determined the average line ratio, weighted by the uncertainty in the line flux measurements, for all of the stars in our sample. In addition, we calculated the weighted standard deviation from the mean to estimate the scatter in this measurement. In Figure 2, we plot a solid line whose slope is the ‘global’ line ratio for $\text{Pa}\gamma/\text{Pa}\beta$, while the dashed line represent the scatter measurement.

Although not shown here, similar linear relationships were found for the rest of the HI emission features observed and ‘global’ line ratios were determined for those using the same method. Each ratio uses the Paschen or Brackett series transition with the lowest excited state as the reference transition ($\text{Pa}\beta$ with $n_u = 5$ and $\text{Br}\gamma$ with $n_u = 7$). In the case of the Paschen series, eight emission lines were ratioed with the reference transition. For the Brackett series, which was weaker and detectable only in the most active TTS, we measured seven emission features. The number of stars possessing measurable emission at the higher transitions in the Brackett series diminished quickly with the highest three

transitions being observed only in a few epochs of DR Tau. Having determined a set of line ratios for both the Paschen and Brackett decrements, it is possible to make a direct comparison between the observed decrements, *not a single ratio*, and the decrements predicted by Case B and the optically thick and thin LTE regimes.

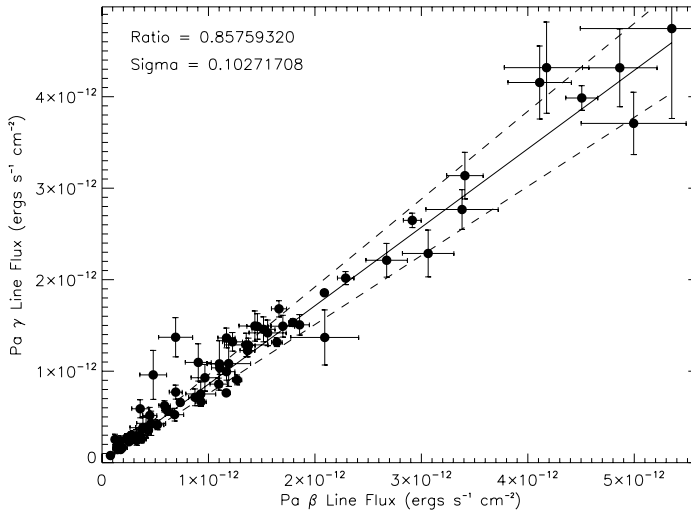


Figure 2. For each spectra in our sample, we plot the measured Pa β line flux versus that measured for Pa γ with associated errors and find a strong linear correlation between these emission features. The solid line plot through the data has a slope equal to the weighted average of the data points. The dashed lines represent the weighted standard deviation and provide a useful measure of the scatter about the weighted mean.

5. Case B comparison

We used the fortran program provided by Storey & Hummer (1995) (on-line at <http://vizier.u-strasbg.fr/viz-bin/VizieR?-source=VI/64> and accompanied by the necessary data files) to produce models of the Paschen and Brackett decrements as well as the line ratios of Br γ to Pa n for 130 different temperature and electron density combinations for $500 \leq T \leq 30000$ K and $100 \leq n_e \leq 10^{14}$ cm $^{-3}$. We calculated the reduced Chi-squares to determine which, if any, models were good fits to our data.

In Figure 3, we plot a line ratio curve for the observed Paschen decrement using Pa β as the reference transition and overplot the four Case B models with the smallest χ^2 values. The ‘scatter’ bars on each of the data points represent the weighted standard deviation discussed in §4. The closest model (the one with the smallest χ^2) has a temperature of 1000 K and an electron density of 10^{10} cm $^{-3}$ and a reduced χ^2 of 0.89. A similar comparison was made for the Brackett decrement and the closest model was determined to have $T = 500$ K, $n_e = 10^{10}$ cm $^{-3}$, and $\chi^2 = 0.43$. The fact that the closest Case B models to fit the Paschen and Brackett series independently have the similar T and the same n_e is strong evidence that the assumptions of Case B theory approximate the conditions in the emitting gas.

We proceed with a comparison of line ratios between the Paschen series and the strongest Brackett feature, Br γ . The large separation in wavelength between the Paschen series and Br γ allows us to search for any dependence in our Case B comparison on the

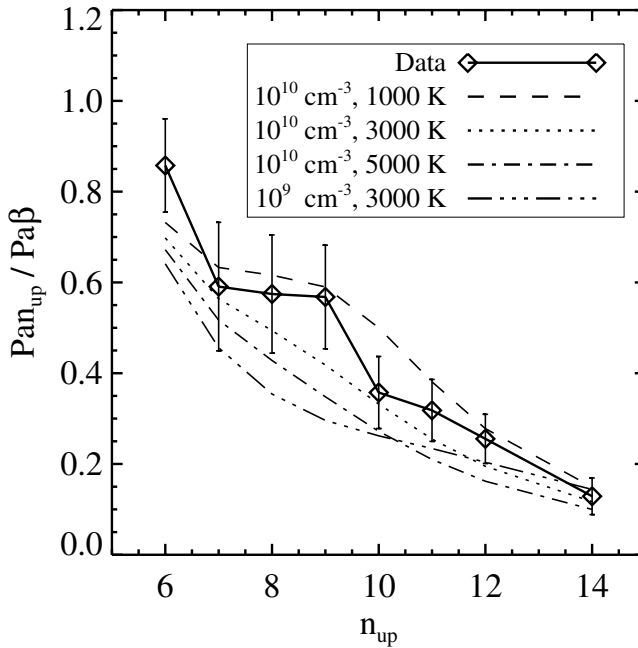


Figure 3. We plot the weighted mean $Pan/Pa\beta$ ratio versus the principal quantum number, n , of the upper level as a solid line connecting the diamond-shaped data points. ‘Scatter’ bars, determined from the weighted standard deviation from the mean line ratio value, are plotted on top of the data points. Of the possible 130 models, we overplot the four models with the smallest reduced χ^2 values. The temperatures and electron densities for these models are given in the figure legend.

reddening correction. In Figure 4, we present the line ratio curve for $Br\gamma$ to Pan including the closest model with $T = 10^3$ K and $n_e = 10^{10}$ cm^{-3} . We overplot four additional Case B line ratio curves holding the temperature constant ($T = 1000$ K) and using four densities in the Storey & Hummer (1995) grid of models adjacent to the density of the best fit. At low n -values, the spread in predicted line ratios is quite small for this temperature. However, for the line ratios of the n_{upper} states of the Paschen transitions, the models separate quite well, clearly distinguishing the model that most closely matches data. As a result, the $Br\gamma$ to Pan line ratios place a strong constraint on n_e of the emitting gas. Again, the temperature and density of the closest Case B model for $Br\gamma/Pan$ agree well with those determined for both the Paschen and Brackett decrements. This result suggests that the spectra were properly corrected for reddening.

6. LTE optically thick and thin

In Figure 5, we compare the observed $Br\gamma$ to Pan line ratio curves to those predicted by both an optically thick ($\tau \gg 1$) and thin ($\tau \ll 1$) region of H I gas. We find no correlation between the LTE line ratios and the measured line ratios for any temperature, with the exception of the $Br\gamma$ to $Pa\delta$ line ratio. Since both transitions begin with the $n = 7$ principal quantum state, the line ratio in the optically thin limit is temperature independent. For the densities considered here, the Case B ratio approaches the same value as in the LTE optically thin case. The fact that our observed value of $Br\gamma/Pa\beta$

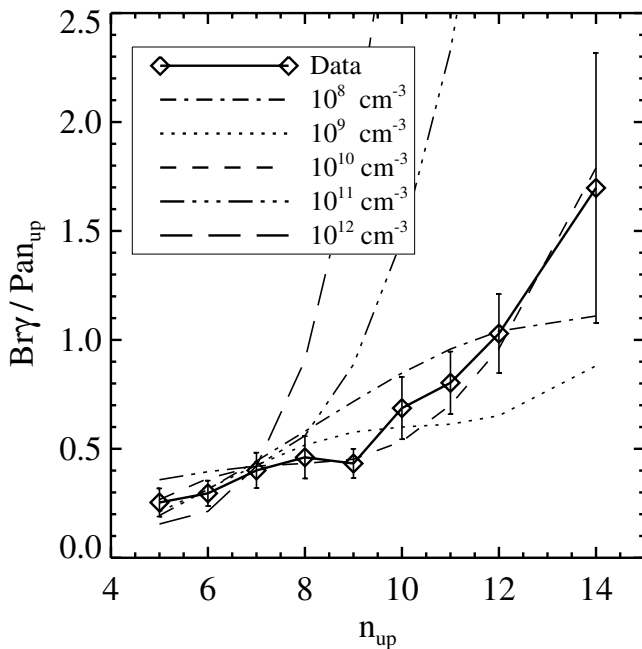


Figure 4. We plot the values of the line ratios of Br γ to the Paschen series. The broad wavelength coverage between the Brackett and Paschen lines provides a stronger constraint on density as the predicted ratios diverge significantly at high n . We demonstrate this sensitivity by plotting four models of constant temperature ($T = 10000$ K) and separated by one order of magnitude in density along with the data. Once again, we find the model with the smallest Chi-square is $n_e = 10^{10} \text{ cm}^{-3}$.

matches both the LTE optically thin and the Case B value is independent evidence that these two lines are optically thin.

As the temperature increases for the optically thin case, the curves quickly approach an asymptotic limit and will never match the observed line ratio curve. As for the optically thick cases, two curves are plotted that bracket the previously predicted temperatures for the accreting gas (≈ 6000 – 12000 K: Martin 1996; Muzerolle *et al.* 1998a) and clearly do not fit the shape of the observed values. Figure 5 clearly rules out both the LTE optically thin and thick cases for the emitting HI lines.

7. Conclusions

In contrast to previous comparisons of observed HI line ratios to those predicted by Case B approximation in line recombination theory, we find good agreement to our observed values for a tightly constrained range of T and n_e . We do not find any agreement between our observed values and those predicted for the optically thick and thin LTE cases suggesting that the level populations are *not* in LTE. Therefore, we conclude that the emitting gas is optically thin to the detected infrared HI lines and that the bulk of this line emission is produced in a non-LTE recombining gas with $T < 5000$ K and $n_e \approx 10^{10} \text{ cm}^{-3}$ (see Figure 6).

Does the emission originate in the accretion flow? The measured temperature range is far lower than the $T = 10^4$ K previously predicted for gas confined to an accretion

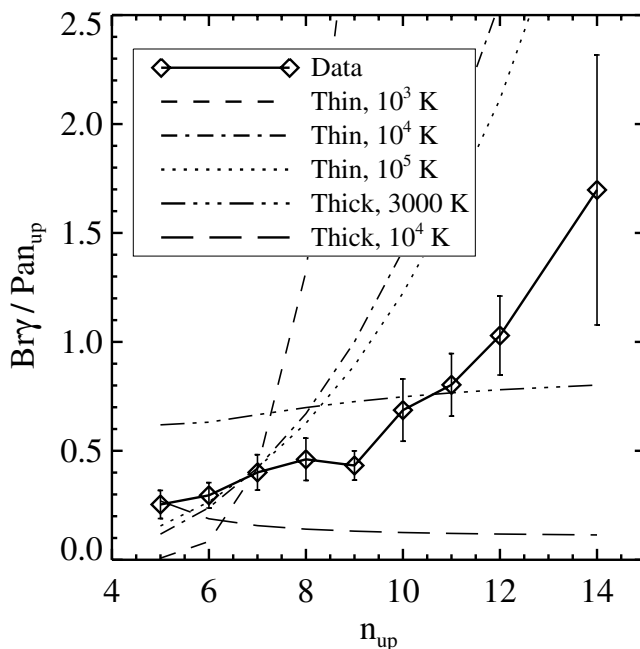


Figure 5. We plot the values of the line ratios of Br γ to the Paschen series as a solid line connecting the measured line ratios. ‘Scatter’ bars, determined from the weighted standard deviation from the mean line ratio value, are plotted on top of the data points. Overplotted are models for the LTE optically thick and thin cases for a variety of temperatures consistent with those expected for gas in an accreting column. In the optically thin limit, one model with a temperature of 10^5 K is plotted to show the asymptote approached by the LTE models at high T .

flow and would suggest a problem with the incident radiation field or heating vs. cooling rates currently considered in the calculations of the gas temperature. On the other hand, the electron density agrees with the value expected for the neutral hydrogen density of accreting gas (Muzerolle *et al.* 2001) for plausible ionization fractions of 10^{-2} – 10^{-3} . Regardless of its origin, we argue that this Case B analysis makes a strong case that the bulk of the emitting gas is spatially coincident and shares similar emission characteristics. Whether the infrared line emission arises from gas in the accretion flows, at the inner edge of the disk, or in a dense wind flowing away from the star will remain a ‘hotly’ debated issue.

Acknowledgements

J. Bary acknowledges financial support from the NSF Astronomy and Astrophysics Postdoctoral Fellowship program. The research of S. Matt was supported by the University of Virginia through a Levinson/VITA Fellowship, partially funded by The Frank Levinson Family Foundation through the Peninsula Community Foundation. Also, thanks to Phil Arras, Mike Skrutskie, Craig Sarazin, John Wilson, Matt Nelson, & Dawn Peterson for help with the data collection, reduction, and understanding atomic physics.

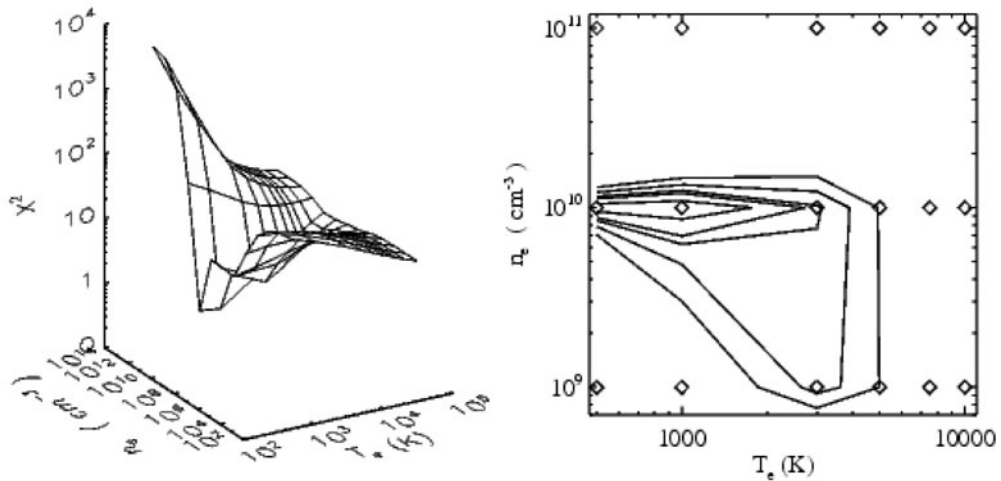


Figure 6. (a) On the left, we plot the reduced χ^2 surface of the 130 density and temperature dependent Case B models provided by Storey & Hummer (1995). The valley of the surface locates models with the smallest χ^2 and approach $T = 1000$ K and $n_e = 10^{10}$ cm^{-3} . (b) On the right, we plot a zoomed in version of the reduced χ^2 contours associated with the 60, 90, 95, 99, & 99.9% confidence intervals on a temperature vs. electron density grid. The empty diamonds designate T_e , n_e grid points from 18 of the 130 Case B models used in our analysis. The contours show the tight constraint placed on densities higher than 10^{10} cm^{-3} . Temperatures greater than 5000 K are ruled out at the 99.9% confidence level.

References

- Alencar, S. H. P., & Basri, G. 2000, *AJ*, 119, 1881
 Baker, J. G., Menzel, D. H., & Aller, L. H. 1938, *ApJ*, 88, 422
 Basri, G., & Batalha, C. 1990, *ApJ*, 363, 654
 Cushing, M. C., Vacca, W. D., & Rayner, J. T. 2004, *PASP*, 116, 362
 Folha, D. F. M., & Emerson, J. P. 2001, *A&A*, 365, 90
 Ghosh, P., & Lamb, F. K. 1979, *ApJ*, 234, 296
 Hartmann, L., Hewett, R., & Calvet, N. 1994, *ApJ*, 426, 669
 Johns, C. M., & Basri, G. 1995, *AJ*, 109, 2800
 Königl, A. 1991, *ApJ*, 370, L39
 Martin, S. C. 1996, *ApJ*, 470, 537
 Muzerolle, J., Calvet, N., & Hartmann, L. 1998a, *ApJ*, 492, 743
 Muzerolle, J., Calvet, N., & Hartmann, L. 2001, *ApJ*, 550, 944
 Muzerolle, J., Hartmann, L., & Calvet, N. 1998b, *AJ*, 116, 455
 Shu, F., Najita, J., Ostriker, E., Wilkin, F., Ruden, S., & Lizano, S. 1994, *ApJ*, 429, 781
 Skrutskie, M. F., Meyer, M. R., Whalen, D., & Hamilton, C. 1996, *AJ*, 112, 2168
 Storey, P. J., & Hummer, D. G. 1995, *MNRAS*, 272, 41